XMM-Newton Observation of Fe Kα emission from a BAL QSO: Mrk 231

T. J. Turner[1,2] & S. B. Kraemer[3]

ABSTRACT

We present results from a 20 ksec *XMM-Newton* observation of Mrk 231. EPIC spectral data reveal strong line emission due to Fe Kα, which has rarely been detected in this class, as BAL QSOs are very faint in the X-ray band. The line energy is consistent with an origin in neutral Fe. The width of the line is equivalent to a velocity dispersion $\sim 18,000$ km s^{-1} and thus the line may be attributed to transmission and/or reflection from a distribution of emitting clouds. If, instead, the line originates in the accretion disk then the line strength and flat X-ray continuum support some contribution from a reflected component, although the data disfavor a model where the hard X-ray band is purely reflected X-rays. The line parameters are similar to those obtained for the Fe Kα line detected in another BAL QSO, H1413 + 117.

Subject headings: galaxies: active – galaxies: individual (Mrk 231) – galaxies: nuclei – galaxies: Seyfert

1. Introduction - the BAL QSO phenomenon

The ejection of matter at moderate to high velocities appears to be a common phenomenon in Active Galactic Nuclei (AGN). Details of the accretion and ejection processes provide fundamental insight into the fueling of the AGN, and the effect of an active nucleus on its environment. Moderate velocity (hundreds of km s^{-1}) outflows have been observed in many Seyfert 1 galaxies (e.g. Kaspi et al. 2002). Broad Absorption Line Quasars (BAL QSOs) are the high-velocity systems, showing blueshifted optical and UV absorption lines from resonant transitions of ionized species such as CIV, SIV, NV and OVI. Fabian (1999) suggested that BAL QSOs are in an early evolutionary phase when the mass of gas around a black hole is beginning to get blown away to reveal a QSO.

The BAL absorption lines are thought to arise in radiatively-driven material along the line-of-sight, with outflow velocities in the range 5000-30,000 km s^{-1} (e.g. Turnshek et al. 1988). BAL QSOs

[1]Joint Center for Astrophysics, Physics Dept., University of Maryland Baltimore County, 1000 Hilltop Circle, Baltimore, MD 21250

[2]Laboratory for High Energy Astrophysics, Code 662, NASA/GSFC, Greenbelt, MD 20771

[3]Catholic University of America, NASA/GSFC, Code 681, Greenbelt, MD 20771

comprise $\sim$ 8% of the high-luminosity QSOs (see Weyman 1997 for an overview). Models for BAL QSOs seek to explain how gas gets accelerated to the observed velocities. Suggestions have included a scenario where gas and radiation pressure lift material from the photosphere of the accretion disk and this gas is illuminated by radiation from the inner disk/corona (Murray et al. 1995). That nuclear photon flux then accelerates the wind outwards. As the inner edge of the wind is thought to be quite close to the central source, some "shielding" gas has been invoked to prevent the wind material becoming stripped, and difficult to drive. This gas is thought to be highly-ionized and have column density in the range $N_H = 10^{22} - 10^{24}\mathrm{cm}^{-2}$. Proga et al. (2000) found that a layer of shielding gas arises naturally in their models for BAL winds. An alternative suggestion is that the outflow consists of dense clouds that are magnetically confined and that have small filling factor (Arav, Li & Begelman 1994).

Constraints to date on the BAL gas location and mass-loss rates have been based on the UV and optical data. X-rays may be the key to understanding BAL QSOs as they offer the opportunity to probe closer to the nucleus than studies in the optical and UV bands. Interesting X-ray results have recently emerged with detection of some broad absorption features from the lensed QSO, APM 082769+5255 (Chartas et al. 2002), indicating an origin in gas components outflowing at $\sim 0.2-0.4$c. However, BAL QSOs are very faint, and detection of significant spectral features in the X-ray band has been rare to date. For example, while Fe Kα emission is commonly seen in Seyfert 1 galaxies (e.g. Nandra et al. 1997) and valued as an indicator of conditions very close to the black hole, this line has been detected in just a few BAL QSOs, e.g. the gravitationally-lensed 'Cloverleaf' QSO, H1413+117 (Oshima et al. 2001). Here we report on a brief *XMM-Newton* (hereafter *XMM*) observation of the BAL QSO Mrk 231, yielding a rare detection of an Fe Kα emission line.

2. The Properties of Mrk 231

Mrk 231 (z=0.042) is an ultraluminous infrared galaxy (ULIRG) and one of the strongest known FeII emitters. Furthermore, Mrk 231 has one of the highest bolometric luminosities in the local ($z < 0.1$) universe with $L_{8-1000\mu m} \sim 4 \times 10^{12} L_{\odot}$ and $L_{BOL} > 10^{46}$erg s^{-1} (Soifer et al. 1987). Bryant & Scoville (1996) find that starburst activity can only account for 40% of the IR luminosity in Mrk 231, an active nucleus appears to provide the rest of the energy. Another extreme property of Mrk 231 is its high polarization, $\sim$ 20% at 2800 Å (e.g. Smith et al. 1995), most likely due to scattering by dust. Broad optical emission lines are observed similar to those defining the Seyfert 1 class. However, no narrow emission lines are seen except for O[II] λ3727. The absence of narrow emission lines is sometimes observed in quasi-stellar objects (QSOs) but rarely in Seyfert galaxies, this, and the high bolometric luminosity of Mrk 231 supported the idea that the nucleus of this source is similar to a QSO. This O[II] emission line is consistent with production in gas which is ionized by hot young stars (Smith et al. 1995) rather than by ultraviolet radiation from the nucleus. This possibility seems attractive since the nuclear UV, extreme-UV and soft X-ray photons are likely to be heavily attenuated by the dense circumnuclear absorber, i.e. the narrow-line gas may not receive ionizing radiation.

Boroson et al. (1991), Rudy et al. (1985) and Rupke et al. (2002) are among those discussing several distinguishable Broad Absorption Line (BAL) systems evident in optical and UV observations of Mrk 231. The most prominent is defined by NaI, CaII and HeI lines originating in gas with an outflow velocity ~ 4200 km s^{-1} relative to the line emission seen in the source. Other systems appear and disappear between observing epochs, showing velocities from ~ 200 km s^{-1} inflow to ~ 8000 km s^{-1} outflow (e.g. Boroson et al. 1991; Kollatschny, Dietrich & Hagan 1992; Forster et al. 1995). Rudy et al. (1985) showed that the shapes of absorption features and velocities in the absorbing gas systems of Mrk 231 are the same as those observed in BAL QSOs and suggested the gas is probably accelerated by the same mechanism. Nevertheless, the nature of the absorbing systems in Mrk 231 continued to be debated. The width of the CIV resonance line is used as a key indicator of the BAL nature of an AGN (Weyman 1997). Heavy reddening has made that line width difficult to constrain in Mrk 231 until an *HST* spectrum settled the case in favor of a BAL QSO designation (Gallagher et al. 2002; hereafter G02). Most BAL systems are dominated by high-ionization species, only $\sim 15\%$ have absorption by low-ionization systems such as MgII$\lambda\lambda$2796 and 2803, AlIII$\lambda\lambda$1671, AlIII$\lambda\lambda$1855 and 1863 and CII$\lambda\lambda$1335 (Voit, Weymann & Korista 1993). In addition to these low-ionization systems, Mrk 231 shows even rarer absorption lines, such as NaID, HeIλ3889 and MgIλ2853. While Mrk 231 does show some of the high-ionization systems (G02) it is dominated by the low-ionization systems; the MgII absorption in particular, places Mrk 231 into the so-called LoBAL subclass of low-ionization BAL QSOs.

2.1. Previous X-ray Observations of Mrk 231

The *ROSAT* High Resolution Instrument (HRI) showed extended soft X-ray emission consistent with the extent of the host galaxy ($\sim 10''$; Turner 1999), confirmed using *Chandra* (G02). An early *ASCA* observation (Iwasawa 1999; Turner 1999) showed a flat spectrum but with insufficient counts to distinguish between absorption or reflection models. In this paper we use the term "reflection" to refer to reprocessing of photons via Compton scattering and fluorescence by material which is optically-thick to electron scattering. We use the term "scattering" to refer to the case where the optical depth to electrons is $0 < \tau < 1$. A longer *ASCA* observation (Maloney & Reynolds 2000; hereafter MR) suggested the X-ray spectrum to be dominated by reflected plus scattered nuclear emission with a large absorbing column in the line-of-sight. Thus MR suggested a Seyfert 2 type geometry and orientation for Mrk 231, with the accretion-disk system surrounded by a thick shell of absorbing gas $N_H \sim 3 \times 10^{22}$cm^{-2} which lies outside of the starburst region (i.e. outside of a radius of $\sim$ 500pc). The latter may be the gas component blocking ionizing radiation from the optical narrow-line region, while allowing hard X-rays to penetrate. G02 find significant variability in the hard X-ray flux, contrary to what is expected in the MR model, and suggested nuclear X-rays are hidden by a Compton-thick cloud (Fig 12 of G02) existing on size-scales $< 10^{15}$cm, while scattered X-rays from multiple lines-of-sight reach the observer. Smith et al. (1995) suggest there may be a superposition of two polarized components in Mrk 231, supporting the importance of scattering in this system.

3. The XMM-Newton Observation

3.1. Data Reduction

An *XMM* observation of Mrk 231 was performed starting 2001 June 7 UT 13:10:24 with an exposure time of $\sim$ 22 ks. Here we present analysis of the archived *XMM* data from that observation. *EPIC* data were processed using SASS 5.4. PN and MOS data utilized the medium filter and the prime full window. The EPIC data were screened to remove hot and bad pixels, and some brief periods of high background counts. Instrument patterns 0 – 12 (MOS) and 0 – 4 (PN) were selected. The screening criteria resulted in an effective exposure of 21.4 ks for the MOS and PN data. The background-subtracted count rates were 0.0391 ± 0.0014 (MOS1), 0.0389 ± 0.0014 (MOS2) and 0.130 ± 0.0028 (PN) over the 0.3-10.0 keV band. Spectra and time series were extracted from a cell of radius $\sim 30''$ centered on the source. Background spectra were extracted from nearby, source-free regions of MOS and PN, the background was $\sim$ 6% of the source count rate. Unfortunately this brief exposure accumulated only 400 source counts in the combined arms of the RGS data, insufficient for spectral analysis.

3.2. EPIC Results

XMM data showed Mrk 231 to have an observed flux $F_{2-10\ keV} \sim 6.2 \times 10^{-13}$erg cm^{-2} s^{-1}, during the June 2001 observation, corresponding to observed luminosity $L_{2-10\ keV} \sim 2 \times 10^{42}$erg s^{-1} (assuming $H_0 = 75$ km s^{-1} Mpc^{-1}, $q_0 = 0.5$ throughout). The 2 - 8 keV flux (5×10^{-13}erg cm^{-2} s^{-1}) is consistent with that reported by G02. We found no significant variations in X-ray flux within this short *XMM* exposure.

The overall spectral shape is complex. Several previous papers have discussed the difficulty in distinguishing between models where the active nucleus is covered by a patchy and/or ionized absorber (Iwasawa 1999; Turner 1999) and those where the spectrum is dominated by a reflected component (MR). This *XMM* exposure is brief and the data do not allow us to determine the precise contributions of reflected and absorbed continua to the overall spectrum. However, progress is possible as the PN spectrum shows two prominent emission lines (Fig 1) plus emission consistent with a blend of lines from the (previously suspected) thermal component peaking between 0.5 - 1 keV (Iwasawa 1999; Turner 1999; Gallagher et al. 2002, MR). EPIC data show some evidence for absorption-like features at $\sim$ 1.1, 1.6 and $\sim$ 2.4 keV. The latter appears only in PN data and is probably an instrumental effect. For the others, the low S/N combined with the modest energy resolution leads to ambiguity between emission and absorption features. These may be absorption features due to Fe, but we cannot be sure.

One of the most obvious features in the PN data is immediately identified with emission from the K-shell of Fe. The PN detects 30 counts in the line during this exposure. The MOS spectra have far fewer counts and the line is not significantly detected in those (although the data are consistent

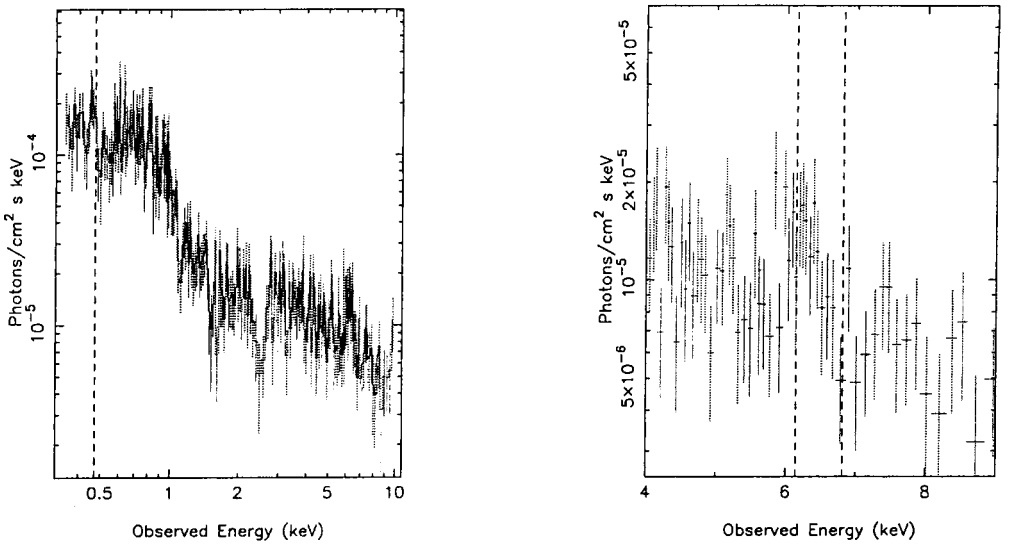

Fig. 1.— *Left: The EPIC PN spectrum of Mrk 231 from a 20 ksec exposure with XMM. A large flux of lines is also evident between 0.5 - 1 keV. A sharp dip just above 2 kev does not show up in MOS data and is likely to be an artifact of the instrument. The dashed vertical line shows where we would expect the* CVI *RRC feature, at the redshift of the host galaxy. The right panel shows a close-up of the Fe Kα line. Dashed lines denote the expected placement of a line emitted at 6.4 keV and an edge at 7.1 keV, observed at the redshift of the host galaxy.*

with the PN results). Thus we used only the PN data to derive the line parameters given below.

First we fit the Fe Kα line relative to a 'local' continuum parameterized as an absorbed powerlaw between 4 – 9 keV. (This yielded $\Gamma \sim 1.2$, $N_H \sim 3.9 \times 10^{22}\mathrm{cm}^{-2}$, the flat index is indicative of complex absorption and/or a contribution from reflection, as previously found for this source.) We measured an observed-energy $E = 6.23\pm0.12$ keV, corresponding to a rest-energy $E = 6.49\pm0.12$ keV correcting for the systemic velocity of the host galaxy. The line width was $\sigma = 0.17^{+0.12}_{-0.11}$ keV with flux $n = 3.85^{+2.11}_{-1.86} \times 10^{-6}$ photons cm^{-2} s^{-1} and the luminosity in the line was $L_{FeK} = 1.3 \times 10^{41}$erg s^{-1}. The lower limit of $\sigma = 60$ eV means the Fe Kα line has a significant breadth. The line equivalent width is $\sim 450^{+229}_{-204}$ eV relative to the powerlaw continuum. Errors are 90% confidence. For comparison the spectral resolution of the PN at 6.4 keV is $\sigma \sim 50$ eV. Fig 1 shows the data compared to lines denoting the expected observed energies of an emission line from neutral Fe, along with the energy of the Fe K edge which would arise in the same gas, both assumed to be observed at the redshift of the host galaxy. While a dip is evident at the energy where an edge is expected, addition of an edge did not improve the fit significantly.

For comparison, we fit the line relative to a "pure reflection" model for data in the 2 - 10 keV band (as suggested by MR). This fit utilized the PEXRAV model (Magdziarz & Zdziarski 1995) from XSPEC. Fits were attempted assuming disk inclination angles of 45° and 0° (face-on). The (unseen) powerlaw was inferred to be steep with $\Gamma \sim 2.6$ and assumed to turn-over at 100 keV. Fits using either disk orientation gave a line equivalent width ~ 200 eV relative to the reflected continuum. The equivalent width is lower than that found relative to the absorbed powerlaw because the edge

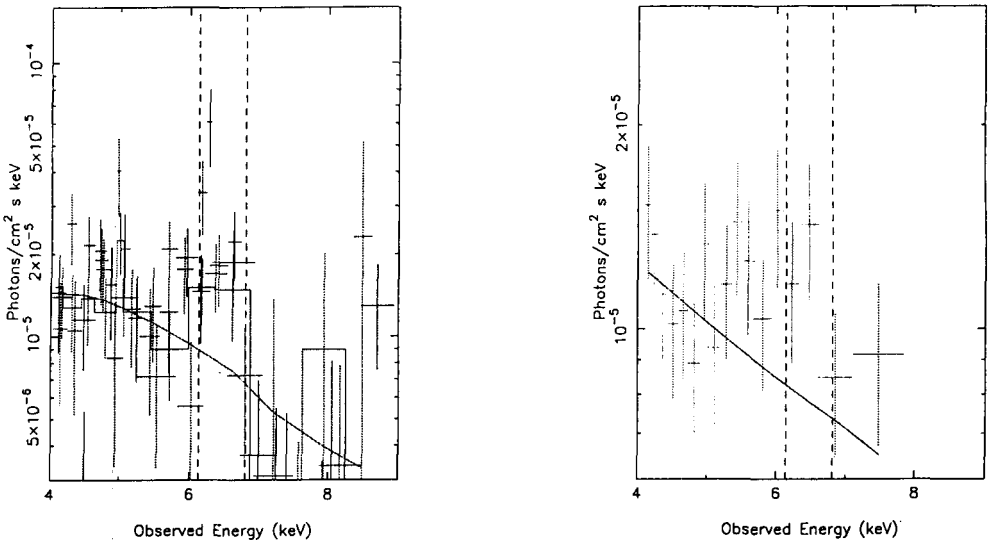

Fig. 2.— *The left-hand panel the Fe Kα line in the combined instruments provided by ASCA data, the dashed vertical lines represent the energies of a line at 6.4 keV and an edge at 7.1 keV observed at the redshift of the host galaxy. The right-hand panel shows data in the same regime from our analysis of the archived ACIS observation of 2000 October. The Fe Kα line is evident in both datasets, and the flux is consistent with that found by the PN*

in the reflected continuum contributes to the curvature just above 6.4 keV, and so fewer photons are attributed to the line. In these two (pure reflection) disk models the line is about 10% of the strength expected, relative to the reflected continuum (George & Fabian 1991). Thus the line strength is low compared to the model in this picture. As the discrepancy is in the ratio of reflected line to reflected continuum, we can extend this result to a range of geometries. The line is too weak relative to the reflected continuum if reflection occurs from either a disk or a distribution of clouds.

To confirm the presence of this line, and look for flux variability we reduced the long archival observation by *ASCA*, from 1999 November 10-12. Data reduction followed the methods outlined for the Tartarus database (Turner et al. 2001). The *ASCA* spectral data were fit using all four instruments, and the spectrum confirms the presence of the Fe line (Fig 2). The spectrum was modeled, constraining photon index, absorption, line energy and line width to match the values derived from the *XMM* data. This produced a good fit, with continuum flux $F_{2-10\ keV} \sim 7.5 \times 10^{-13}$erg cm^{-2} s^{-1} and line flux $n = 5.76^{+2.91}_{-2.78} \times 10^{-6}$ photons cm^{-2} s^{-1}.

We also reduced the archived ACIS data from 2000 October 19-20, originally reported by G02 (Fig 2). Extracting ACIS CCD spectra of Mrk 231 we fit the data using the same continuum and line model used for the *XMM* and *ASCA* spectra, leaving only line and continuum normalizations free. This model yielded a line flux $n = 2.48^{+2.26}_{-2.25} \times 10^{-6}$ photons cm^{-2} s^{-1}. The differences in line flux are not significant and so the data show the line flux to be consistent with a constant value over a baseline of 1.5 years.

Turning to the soft X-ray band. Previous PSPC (Turner 1999) and *Chandra* ACIS data (G02)